Applied Surface Science 256 (2010) 6717–6722

Contents lists available at ScienceDirect

Applied Surface Science

journal homepage: www.elsevier.com/locate/apsusc

Solvent effects on adsorption of CO over CuCl(1 1 1) surface: A density functional theory study

Riguang Zhang, Lixia Ling, Baojun Wang*, Wei Huang

Key Laboratory of Coal Science and Technology of Ministry of Education and Shanxi Province, Taiyuan University of Technology, Yingze West Street No 79, Taiyuan 030024, Shanxi, China

ARTICLE INFO

Article history:
Received 25 November 2009
Received in revised form 21 March 2010
Accepted 20 April 2010
Available online 28 April 2010

Keywords:
Carbon monoxide
CuCl(1 1 1)
Solvent effects
Adsorption
Density functional theory

ABSTRACT

DFT calculations have been performed to investigate the effect of dielectric responses of the solvent environment on the CO adsorption over CuCl(1 1 1) surface by using COSMO (conductor-like solvent model) model in Dmol^3. Different dielectric constants, including vacuum, liquid paraffin, methylene chloride, methanol and water solution, are considered. The effects of solvent model on the structural parameters, adsorption energies and vibrational frequency of CO adsorption over CuCl(1 1 1) surface have been investigated. The calculation results suggest that solvent effects can improve the stability of CO adsorption and reduce the intensity of C–O bond, which might mean that solvent is in favor of C–O bond activation and improve the reaction activity of oxidative carbonylation in a slurry reactor.

1. Introduction

Dimethyl carbonate (DMC) has drawn continuous attention from researchers due to its applications in replacing environmentally unfriendly compounds [1]. The oxidative carbonylation of methanol to DMC has received more attention than the other processes of making DMC because its raw materials are abundant and inexpensive, and its process is environmentally friendly. Nowadays, there are two methods of "one-pot" synthesis of DMC: the gas phase method and the liquid phase method. The gas phase method generally uses a fixed bed reactor [2]. While the liquid phase method uses a slurry reactor [3].

It is well known that Cu$^+$ ions have been postulated to be the active species for the formation of DMC by the oxidative carbonylation of methanol [4,5]. And cuprous chloride (CuCl) is zincblend-structured material and is particularly appealing because of its unusual electrical and lattice-vibration properties and intriguing host–impurity interaction [6]. Besides, CuCl(1 1 1) polar surface is an ideal unrelaxed surface [7,8], and three coordinated unsaturated Cu(I) sites on CuCl(1 1 1) surface have been proposed as the active centers for the high activity catalysts [9]. So in our previous works [10–12], DMC is mainly produced by the oxidative carbonylation of methanol on CuCl catalyst in a slurry reactor. However, this process often falls into severe equipment corrosion and catalyst deactivation. As a result, several efforts for DMC synthesis have been made to develop new and more efficient catalyst systems using various base additives [13–15] or ionic liquids [16] as promoters or co-solvents. In these systems, CuCl is used as catalyst, and suspended in the methanol, water and other liquid phase solvent. Then, gas reactant CO adsorbs on the CuCl and interacts with the active center of the CuCl in the liquid phase. Anderson et al. [4,5,17] and Bell et al.'s [18,19] studies indicated that CO addition to adsorbed methoxide species to form carbomethoxide species was proposed to be the rate-limiting step, CO adsorption and activation on Cu$^+$ catalyst is very important for the addition reaction. In addition, Romano et al.'s experimental results [20] shown that water in reaction system can catalyze the CO oxidation to CO_2 well and enhance the ability of CO activation. Zuo et al.'s studies [21] have shown that the C–O bonds in liquid paraffin are longer than the C–O bonds in vacuum, which might mean that the liquid solvent can improve the CO activation, the formation of DME from syngas ($CO + H_2$) conversion uses the liquid phase method in a slurry reactor, where the catalyst is dispersed in a liquid medium such as liquid paraffin [22–25], In other words, the syngas ($CO + H_2$) conversions, such as the DME synthesis, could be improved in a slurry reactor.

Although the chemical environment of Cu$^+$ ions differs from that of Cu$^+$ ions in CuCl(1 1 1), information about the interaction of CO with CuCl(1 1 1) surface contributes to understanding the interaction of CO with the unsaturated Cu$^+$ ions. Based on the above facts, for the formation of DMC by the oxidative carbonylation of methanol in a slurry reactor, it is significant to investigate the

---

* Corresponding author. Fax: +86 351 6018539.
E-mail address: wangbaojun@tyut.edu.cn (B. Wang).

0169-4332/$ – see front matter © 2010 Elsevier B.V. All rights reserved.
doi:10.1016/j.apsusc.2010.04.079

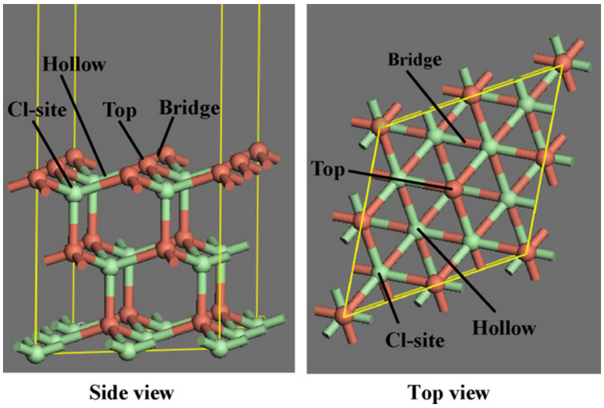

Side view Top view

Fig. 1. The slab model of CuCl(1 1 1)-(2 × 2) supercell (top view and side view). Blue balls represent Cl atoms and orange balls represent Cu atoms. (For interpretation of the references to color in this figure legend, the reader is referred to the web version of the article.)

effect of liquid solvent on the adsorption of CO over CuCl(1 1 1) surface using a solvent model. Up to date, the adsorption of CO over CuCl(1 1 1) surface in vacuum has been studied by researchers [6,8,26]. No studies have been reported about solvent effect on the adsorption of CO over CuCl(1 1 1) surface. So the Dmol^3 implementation of the COSMO (conductor-like solvent model) is applied to simulate the dielectric response of the solvent environment [21,27,28]. And COSMO model has been used in our previous studies about the solvent effects on the CO adsorption over Cu($h\,k\,l$) surface [21] and Cu_2O(1 1 1) surfaces [29]. In our present study, values of the solvent dielectric constants ε ranging from 2.06 (liquid paraffin) to 78.54 (water) were considered, including 9.08 (methylene chloride) and 32.63 (methanol). COSMO has not been used in vacuum ($\varepsilon = 1$).

The main question addressed in this study is “to what extent is the solvent as a continuum affecting the relative stability, structure and vibrational frequencies of the CO adsorption over CuCl(1 1 1) surface?”. And the specific questions is “what is the solvent influence on the intensity of the C–O bond in different solvents?”. These questions will be herein addressed within the framework of COSMO–based DFT.

2. Computation method and model

2.1. Computation details

The exchange and correlation effects are described through the generalized gradient approximation (GGA) of Becke–Lee–Yang–Parr (BLYP). The double-numeric basis with polarization functions (DNP) is used for all atoms in the adsorbed and substrate systems. All electron basis set is used for C, O and Cl atoms, and effective core potentials (ECP) are used for Cu atoms. The converge criterion judged by the energy, force and displacement, respectively, are 2×10^{-5} Ha, 4×10^{-3} Ha/Å, 5×10^{-3} Å. The k-point sampling scheme of Monkhorst–Pack grid of $4 \times 4 \times 1$ and Methfessel–Paxton smearing of 0.005 hartree were utilized. All calculations were carried out with the Dmol^3 program package in Materials Studio (version 4.4) [30,31].

2.2. Surface models

CuCl has a face-centered cubic structure with its cell parameter $a = 0.5406$ nm, in which the Cu and Cl atoms adopt the form of tetrahedral coordination. In our study, the CuCl(1 1 1) surface is adopted to study the adsorption properties [32]. Fig. 1 shows the CuCl(1 1 1)-(2 × 2) supercell mode including six atomic layers. Four different adsorption sites are selected: top, bridge, hollow and Cl-site on CuCl(1 1 1) surface. The top is three coordinated unsaturated Cu(I) sites, the Cl-site is above one of the Cl atoms of the first layer, and the hollow site is above one of the Cl atoms of the second layer, as shown in Fig. 1 (the side and top view of CuCl(1 1 1) surface). The vacuum space of 1.0 nm was inserted in the direction perpendicular to the surface in order to prevent interactions between periodic images. No relaxation or reconstruction has been observed according to the experimental results [6,8]. Therefore, during the geometry optimizations, the adsorbed CO molecule is allowed to relax and the substrate is fixed as it is in the bulk geometry.

Table 1
Bond length, bond dissociation energy and stretching frequency for free CO molecule.

Method	$d_{(C-O)}$ (nm)	BDE (kJ mol^{-1})	ν_{C-O} (cm^{-1})
GGA-BLYP	0.1143	1091.24	2128
Exp.	0.1128 [35]	1076.38 ± 0.67 [36]	2138 [37]

Note: $d_{(C-O)}$, BDE and ν_{C-O} represent the C–O bond length, bond dissociation energy and C–O bond stretching frequency, respectively.

3. Result and discussion

In order to verify the credibility of the selected calculation method, the bond length, stretching frequency and bond dissociation energies (BDE) of CO molecule have been calculated and listed in Table 1. In addition, the calculated value for the lattice constant of CuCl is 0.5602 nm. The largest deviations from the equilibrium lattice constant 0.5406 nm [32] are around 3.60%. Above results suggest that the calculated equilibrium lattices constant are in agreement with the experimental results.

3.1. Surface energies of CuCl(1 1 1) surface

For surface energies of CuCl(1 1 1) surface calculated in vacuum [33,34]:

$$E_{suf} = \frac{E_{CuCl(1\,1\,1)} - E_{bulk}}{2S_{CuCl(1\,1\,1)}} \qquad (1)$$

where E_{suf} is the surface energy of CuCl(1 1 1) surface, $E_{CuCl(1\,1\,1)}$ and E_{bulk} are the total energy of CuCl(1 1 1) surface in vacuum and the bulk phase of CuCl containing the same number of atoms as in the slab, and $S_{CuCl(1\,1\,1)}$ is the surface area of CuCl(1 1 1) surface. The surface energies E_{suf} in other environments are also used by Eq. (1).

According to Eq. (1), the surface energies in different environments are reported in Fig. 2. As shown in Fig. 2, it can be seen that the surface energies of CuCl(1 1 1) decrease as the dielectric constants increase. When dielectric constants change from vacuum (1) to methylene chloride (9.08), the values of surface energies change rapidly. However, when the dielectric constant is equal to or greater than 32.63, the changes on the surface energies are not obvious.

For a nanocrystallite of a given volume, the Gibbs–Curie–Wulff law [34] allows the morphology to be determined according to the following relationship:

$$\frac{E_{suf}}{d_{111}} = \text{constant} \qquad (2)$$

where $d_{1\,1\,1}$ is the length of the normal line to the 1 1 1 face from Wulff's point in the crystal. On the other hand, the pyramid with the base of the 1 1 1 face and the height of $d_{1\,1\,1}$ has a volume as:

$$V = \frac{S_{CuCl(1\ 1\,1)} d_{1\,1\,1}}{3} \qquad (3)$$

And the total volume is held tightly.

According to Eqs. (2) and (3), it can been seen that the smaller the surface energies, the larger the surface area, so the CuCl(1 1 1)

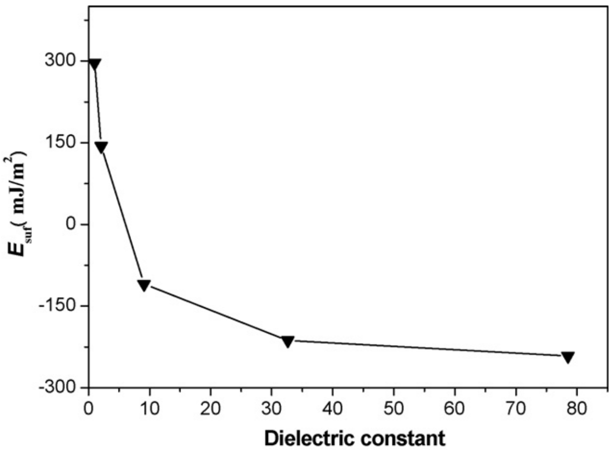

Fig. 2. The surface energies of CuCl(1 1 1) surface with different dielectric constants.

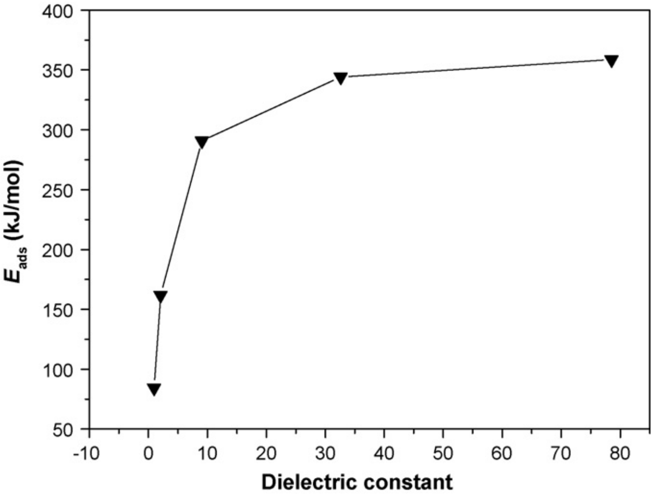

Fig. 3. The change of the adsorption energy for CO adsorbed at the top site of CuCl(1 1 1) surface with variable dielectric constant of the solvent.

surface area in solvents is larger than that in vacuum. Namely, when dielectric constants change from vacuum (1) to methylene chloride (9.08), surface area change rapidly, and stable for higher values of $\varepsilon = 32.63$. The above result shows that solvent environment favors CuCl(1 1 1) surface area growth, which may be propitious to the adsorption of CO over CuCl(1 1 1) surface [34]. However, whether the solvent improve the stability of CO adsorption and the ability of CO activation, we will calculate the adsorption of CO over CuCl(1 1 1) in vacuum and solvent.

3.2. CO adsorption over CuCl(1 1 1) in vacuum

The adsorption energy is given by $E_{ads} = (E_{CO} + E_{CuCl(111)}) - E_{CO/CuCl(111)}$, where E_{ads} is the adsorption energy of the CO molecule over CuCl(1 1 1) surface, $E_{CO/CuCl(111)}$ is the total energy of the optimized relaxed CO over CuCl(1 1 1) surface, E_{CO} is the total energy of the CO molecule, and $E_{CuCl(111)}$ is the total energy of the fixed CuCl(1 1 1) slab. Hence, a more positive adsorption energy indicates a more favorable structure.

The adsorption of CO molecule over CuCl(1 1 1) surface in vacuum was firstly studied, with the molecule vertical over four different adsorption site, top, bridge, hollow and Cl-site, with both the oxygen and carbon ends of the CO molecule closer to the surface [26]. The label O-down and C-down considered in this work denote the model, which CO molecule adsorbs on different site with O end and C end, respectively. $d_{(C–O)}$, $d_{(Cu–X)}$, α and $q_{(CO)}$ represent the C–O bond length, the adsorbed distances, the angle between adsorbed site and CO molecule and the net charge of CO after adsorption, respectively. The calculated results are summarized in Table 2.

For O-down molecular orientation, CO is found to have a tendency to leave the surface, as for the four adsorption models, their adsorption energies are all relatively small ($E_{ads} < 40\,\text{kJ mol}^{-1}$, see Table 2), which is indicative of a physisorption. For C-down molecular orientation, the adsorption models of the bridge and Cl-site are shown to migrate to the hollow and top site after optimization, respectively. So Table 2 lists the parameters of CO adsorption on the hollow and top site. It can be observed that the maximum adsorption energy is obtained when CO is above the top site of CuCl(1 1 1) surface, and the corresponding adsorption energy is 84.5 kJ mol^{-1} ($E_{ads} > 40\,\text{kJ mol}^{-1}$, a chemisorption), indicating that CO prefers to adsorb at the top site. Moreover, the adsorption model has the minimum adsorbed distances 0.2130 nm, the smaller the adsorbed distance is, the more stable the adsorption system is, that is in good agreement with the result deduced from the adsorption energy. Casarin et al. [6] reported a higher value of 150.6 kJ mol^{-1} for the adsorption energy of the CO over CuCl(1 1 1) surface using a molecular cluster approach. The difference in the two values is likely an effect of the finite size of the CuCl cluster used in their model. Cluster calculations typically predict stronger binding energies than periodic slab models. The adsorption energy of CO over CuCl(1 1 1) surface using variable photon energy photoelectron spectroscopy (PES) [8] is 96.2 kJ mol^{-1}, which is about 11.7 kJ mol^{-1} higher than our calculated result. The C–O bond length is 0.1150 nm, which is longer than the corresponding length for the free CO molecule that is found to be 0.1143 nm (the experimental value [35] is 0.1128 nm). This indicates that the intensity of C–O bond is weakened. The electron transfer from CO to substrate as the C atom bound to top site and the net charge of CO is 0.079*e*. Therefore, CO with C-down adsorbed at the top site of the CuCl(1 1 1) surface is the most stable chemisorption structure.

3.3. CO adsorption over CuCl(1 1 1) in solvent

3.3.1. Structural parameters differences

In order to investigate more deeply the effect of the solvent, the CuCl(1 1 1) surface adsorbing CO in four types of solvents, such as liquid paraffin, methylene chloride, methanol and water, were studied. The calculated results show that the adsorption models of bridge and Cl-site still migrate to that of hollow and top site after optimization, respectively. The top site is still the preferred adsorption site of CO over CuCl(1 1 1) surface. So we will focus the CO adsorption on the top site of the CuCl(1 1 1) surface in solvent. Table 3 presents the values of the most relevant structural parameters for the stable structure of CO adsorbed at the top site. Adsorption energies are plotted in Fig. 3 as functions of the solvent dielectric constant. In this figure, all the adsorption models are stabilized when the solvent dielectric constant increases. In the considered range of ε (from 1 for vacuum, to 78.54 for water), vacuum is stabilized by 84.5 kJ mol^{-1}, liquid paraffin by 161.9 kJ mol^{-1}, methylene chloride by 290.8 kJ mol^{-1}, methanol by 344.2 kJ mol^{-1} and water by 358.7 kJ mol^{-1}. These adsorption energies vary mainly for dielectric constant values up to $\varepsilon = 9.08$, remaining small change for higher values. The above result shows that the solvent can promote the stability of CO adsorption over CuCl(1 1 1) surface.

The following general trends can be drawn from Table 3 and Fig. 4. The C–O and Cu–C bond lengths are plotted in Fig. 4 as functions of the solvent dielectric constant. As shown in Fig. 4(a), the C–O bond length increases when ε varies from 1 to 9.08, stable for higher values of $\varepsilon = 32.63$. The C–O bond length is the maximum for dielectric constant value up to $\varepsilon = 9.08$. This result indicates that solvent induce the higher activation of C–O bonds than that in vacuum

Table 2
Predicted geometrical parameter, the adsorption energies and Mulliken charge at different adsorption sites of CuCl(1 1 1) surface in vacuum.

Parameters[a]	O-down				C-down	
	Top	Cl-site	Bridge	Hollow	Top	Hollow
$d_{(C–O)}$ (nm)	0.1145	0.1145	0.1145	0.1146	0.1150	0.1158
$d_{(Cu–X)}$ (nm)	0.3905	0.4383	0.4097	0.4135	0.2130	0.2816
α (°)	179.72	179.52	164.94	179.82	172.50	179.95
$q_{(CO)}$	−0.005	−0.005	−0.005	−0.005	0.079	−0.093
E_{ads} (kJ mol^{-1})	11.2	10.9	11.1	11.1	84.5	19.0

[a] $d_{(C–O)}$, $d_{(Cu–X)}$, α and $q_{(CO)}$ stand for the C–O bond length, the adsorbed distances, the angle between adsorbed site and CO molecule and the net charge of CO after adsorption.

Table 3
Calculated geometrical structural, adsorption energy and the net charge of CO adsorbed at the top site of CuCl(1 1 1) surface in different solvents.

Parameters	Vacuum	Liquid paraffin	Methylene chloride	Methanol	Water
$d_{(C–O)}$ (nm)	0.1150	0.1158	0.1163	0.1161	0.1161
$d_{(Cu–C)}$ (nm)	0.2130	0.1935	0.1933	0.1913	0.1907
α (°)	172.50	179.7	179.5	179.6	179.8
$q_{(CO)}$	0.079	0.123	0.093	0.124	0.133
E_{ads} (kJ mol^{-1})	84.5	161.9	290.8	344.2	358.7

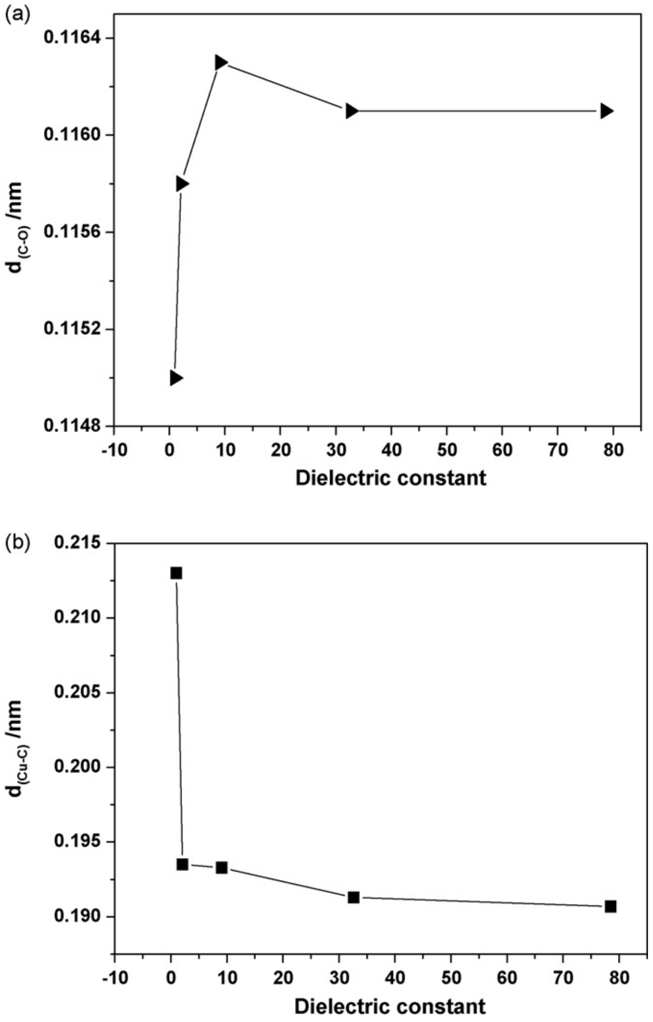

Fig. 4. The C–O and Cu–C bond length change for CO adsorbed at the top site of CuCl(1 1 1) surface with variable dielectric constant of the solvent.

and weaken the intensity of C–O bond. And the Cu–C bond length decreases when ε varies from 1 to 9.08, stable for higher values of ε (see Fig. 4(b)). The smaller the Cu–C bond length is, the more stable the adsorption system is, which is in good accordance with the results obtained from the adsorption energy. In solvent, the bond angle α changes little. The above calculated results show that the solvent not only increase the chemisorption energies but also influences the C–O and Cu–C bonds. The net charge of the chemisorbed CO over CuCl(1 1 1) surface given in Table 4 can be compared with those of free CO molecule. This shows clearly that the chemisorbed CO molecules are positively charged, and the electron transfer from CO to CuCl(1 1 1) surface. With the increase in dielectric constant ε of solvent, the net charge increase from 0.079 to 0.133*e*. It is widely accepted that CO binds to metal surfaces via the Blyholder mechanism, in which the bond to the surface is described in terms of the charge donation from the CO 5σ orbital to the surface and the back-donation from the metal to the CO 2π^* orbital, which rationalizes the increase in C–O bond length upon chemisorption [6,35]. Therefore, the elongation of the C–O bond increases with the increase in the net charge of chemisorbed CO molecule. Finally, by using the monitor bonding in Dmol^3, CO adsorbed over CuCl(1 1 1) surface was found to be non-dissociative adsorption in either vacuum or solvent.

3.3.2. *Vibrational frequencies*

The calculated C–O stretching frequency $\nu_{(C–O)}$ for free CO molecule is 2128 cm^{-1}, and the experimental value is 2138 cm^{-1} [37], which suggests that the error exists between the calculated and experimental value. So emendation factor $\alpha = \nu/\nu_0$ [38] was used to revise the calculated C–O stretching frequency, where ν_0 is the experimental value of C–O stretching frequency, $\nu_0 = 2138$ cm^{-1}; ν is the calculated C–O stretching frequency. Table 4 presents the C–O stretching vibrational frequencies in vacuum and different solvents.

In Table 4, A red-shift (89 cm^{-1}) is observed for CO adsorption over CuCl(1 1 1) surface in vacuum, The red-shift (38 cm^{-1}) of $\nu_{(C–O)}$ upon coordination of CO over CuCl(1 1 1) cluster model in vacuum has been reported by Casarin et al. [6]. With the dielectric constants ε increasing, the C–O stretching frequency decreases by 183, 227, 210 and 208 cm^{-1} for liquid paraffin, methylene chloride, methanol and water, respectively. The red-shift of the C–O stretching frequency indicates that the intensity of C–O bond decreases, these results are in good agreement with the results deduced from the C–O bond length. For example, the red-shift (227 cm^{-1}) of the C–O stretching frequency in methylene chloride is the maximum value, which corresponds to the maximum C–O bond length 0.1163 nm (see Table 3).

Table 4
Calculated stretching vibrational frequencies of CO in different solvent systems.

	ν (cm^{-1})		$\Delta\nu$ (cm^{-1})	
	$\alpha = 1$	$\alpha = 0.9953$	$\alpha = 1$	$\alpha = 0.9953$
Free CO	2138	2128	0	0
Vacuum	2049	2039	−89	−89
Liquid paraffin	1954	1945	−184	−183
Methylene chloride	1910	1901	−228	−227
Methanol	1927	1918	−211	−210
Water	1929	1920	−209	−208

Table 5
Adsorption energies of solvent molecules adsorbed at the different sites over CuCl(1 1 1) surface.

Solvent molecules	Adsorption energy E_{ads} (kJ mol^{-1})			
	Top	Hollow	Cl-site	Bridge
Liquid paraffin (C_4H_{10})	27.2	24.2	25.5	25.6
Methylene chloride (CH_2Cl_2)	55.3	55.8	57.1	54.1
Methanol (CH_3OH)	50.2	–	–	36.4
Water (H_2O)	49.2	–	–	36.0

3.4. Solvent molecule adsorption over CuCl(1 1 1)

Considering that solvent molecules may also interact with the CuCl(1 1 1) surface, we investigated the adsorption of solvent molecules over CuCl(1 1 1) surface. For liquid paraffin, as it is a complicated compounds with the main component of linear alkyl C_nH_{2n+2} (n = 18–24), C_4H_{10}, a segment of the linear alkyl C_nH_{2n+2} (n = 18–24), were chosen to study the interaction of liquid paraffin with CuCl(1 1 1) surface. Adsorption energies of solvent molecules in different adsorption sites over CuCl(1 1 1) surface are listed in Table 5. During a full geometry optimization, the CH_3OH and H_2O that are bound to hollow and Cl-site over CuCl(1 1 1) surface are found to readily migrate to top site. As shown in Table 5, the adsorption energy of C_4H_{10} at top site is 27.2 kJ mol^{-1}, which is indicative of a weak physisorption. The adsorptions of other molecules are all very weak chemisorptions.

Combining with the adsorption energy of CO adsorption over CuCl(1 1 1) in solvents listed in Table 3 and that of solvent molecules adsorption over CuCl(1 1 1) in Table 5, we can found that the interaction of solvent molecules with CuCl(1 1 1) surface is far less than that of CO with CuCl(1 1 1) in solvent, which suggests that for the interaction of CO with CuCl(1 1 1) in solvent, solvent molecules, such as liquid paraffin, methylene chloride, methanol and water, primarily play the role of solvent and show strong solvent effects for the adsorption of CO. Therefore, it can be concluded that solvent effect is absolutely dominating cause for the interaction of CO with CuCl in solvent, in which CuCl shows higher catalytic performance for CO activation. But it may be not the only reason promoting carbon monoxide activation.

According to the above chemisorption energy and C–O bond length of CO adsorption over CuCl(1 1 1) surfaces, the ability of CO chemisorption can be obtained in the following order: water ($\varepsilon = 78.54$) > methanol ($\varepsilon = 32.63$) > methylene chloride ($\varepsilon = 9.08$) > liquid paraffin ($\varepsilon = 2.06$) > vacuum ($\varepsilon = 1$). However, the ability of C–O bond activation shows the order: methylene chloride ($\varepsilon = 9.08$) > water ($\varepsilon = 78.54$) ≈ methanol ($\varepsilon = 32.63$) > liquid paraffin ($\varepsilon = 2.06$) > vacuum ($\varepsilon = 1$). Meanwhile, both the structural parameters and the relative energies of CO are very sensitive to the COSMO solvent model. Thus the solvent effects can improve the stability of CO adsorption over CuCl(1 1 1) surface and the ability of CO activation. This analysis gives us some new insights into the understanding of solvent effects.

4. Conclusions

We have studied the effect of different dielectric responses of solvent on the CO adsorption over CuCl(1 1 1) surface. The results mentioned above highlight changes induced by variation of the solvent dielectric constant in three kinds of molecular properties for CO adsorption over CuCl(1 1 1) surface, namely, geometric structure, adsorption energy and vibrational frequency. The stability of chemisorption of CO in solvent is stronger than that in vacuum, which indicates that the solvent effect can improve the ability of CO adsorption. The C–O bond length in solvent is longer than that in vacuum, and the C–O stretching frequency in solvent is smaller than that in vacuum, these results indicate that the solvent can reduce the intensity of the C–O bond, which might mean that the solvent is in favor of the CO activation and improve the reaction activity of oxidative carbonylation in a slurry reactor.

Acknowledgements

The authors gratefully acknowledge the financial support of this work by the National Basic Research Program of China (Grant No. 2005CB221204), and the National Natural Science Foundation of China (Grant Nos. 20906066 and 20976115).

References

[1] P. Tundo, M. Selva, Acc. Chem. Res. 35 (2002) 706.
[2] Z. Li, K.C. Xie, R.C.T. Slade, Appl. Catal. A: Gen. 205 (2001) 85.
[3] U. Romano, R. Tesel, M.M. Mauri, P. Rebora, Ind. Eng. Chem. Prod. Res. Dev. 19 (1980) 396.
[4] S.A. Anderson, T.W. Root, J. Catal. 217 (2003) 396.
[5] S.A. Anderson, T.W. Root, J. Mol. Catal. A: Chem. 220 (2004) 247.
[6] M. Casarin, E. Tondello, A. Vittadini, Inorg. Chim. Acta 235 (1995) 151.
[7] M. Sambi, G. Granozzi, G.A. Rizzi, M. Casarin, E. Tondello, Surf. Sci. 319 (1994) 149.
[8] J.Y. Lin, P. Jones, J. Guckert, E.I. Sokomon, J. Am. Chem. Soc. 113 (1991) 8312.
[9] E.J. Solomon, P.M. Jones, J.A. May, Chem. Rev. 93 (1993) 2623.
[10] Z. Li, F.H. Meng, J. Ren, H.Y. Zheng, K.C. Xie, Chin. J. Catal. 29 (2008) 643.
[11] J. Ren, S.S. Liu, Z. Li, X.L. Lu, K.C. Xie, Appl. Catal. A: Gen. 366 (2009) 93.
[12] J. Ren, Z. Li, S.S. Liu, Y.L. Xing, K.C. Xie, Catal. Lett. 124 (2008) 185.
[13] V. Raab, M. Merz, J. Sundermeyer, J. Mol. Catal. A: Chem. 175 (2001) 51.
[14] J.C. Hu, Y. Cao, P. Yang, J.F. Deng, K.N. Fan, J. Mol. Catal. A: Chem. 185 (2002) 1.
[15] W.L. Mo, H. Xiong, T. Li, X.C. Guo, G.X. Li, J. Mol. Catal. A: Chem. 247 (2006) 227.
[16] W.S. Dong, X.S. Zhou, C.S. Xin, C.L. Liu, Z.T. Liu, Appl. Catal. A: Gen. 334 (2008) 100.
[17] S.A. Anderson, S. Manthata, T.W. Root, Appl. Catal. A: Gen. 280 (2005) 117.
[18] Y.H. Zhang, A.T. Bell, J. Catal. 255 (2008) 153.
[19] X.B. Zheng, A.T. Bell, J. Phys. Chem. C 112 (2008) 5043.
[20] U. Romano, R. Tesei, G. Cipriannni, L. Micucci, Method for the Preparation of Esters of Carbonic Acid, US 4218391 (1980).

[21] Z.J. Zuo, W. Huang, P.D. Han, Z.H. Li, J. Mol. Mode 15 (2009) 1079.
[22] R.T. Figueiredo, A. Martinez-Arias, M.L. Granados, J.L.G. Fierro, J. Catal. 178 (1998) 146.
[23] G. Marbán, A.B. Fuertes, Appl. Catal. B 57 (2005) 43.
[24] G.A. El-Shobaky, A.M. Ghozza, Mater. Lett. 58 (2004) 699.
[25] R.Q. Yang, X.C. Yu, Y. Zhang, W.Z. Li, N. Tsubaki, Fuel 87 (2008) 443.
[26] X. Wang, W.K. Chen, C.H. Lu, Appl. Surf. Sci. 254 (2008) 4421.
[27] E. Tajkhorshid, S. Suhai, J. Mol. Struct. (THEOCHEM) 501–502 (2000) 297.
[28] A. Klamt, G.J. Schürmann, Chem. Soc. Perkin Trans. 25 (1993) 799.
[29] Z.J. Zuo, W. Huang, P.D. Han, Z.H. Li, Appl. Surf. Sci. 256 (2008) 2357.
[30] B. Delley, J. Chem. Phys. 92 (1990) 508.
[31] B. Delley, J. Chem. Phys. 113 (2000) 7756.
[32] N.C. Baenziger, S.L. Modak, C.L. Fox, J. Acta Crystallogr. C 39 (1983) 1620.
[33] P. Raybaud, M. Digne, R. Iftimie, W. Wellens, P. Euzen, H. Toulhoat, J. Catal. 201 (2001) 236.
[34] Z.J. Zuo, L.L. Sun, W. Huang, P.D. Han, Z.H. Li, Appl. Catal. A: Gen. 375 (2010) 181.
[35] J.X. Shao, X.L. Chen, X.D. Yang, F.P. Zhang, S.H. Ge, J. At. Mol. Phys. 23 (2006) 80.
[36] Y.R. Luo, Handbook of Chemical Bond Dissociation Energies, Science Press, Beijing, 2005, p. 209.
[37] B.Z. Sun, W.K. Chen, J.D. Zheng, C.H. Lu, Appl. Surf. Sci. 255 (2008) 3141.
[38] B.Z. Sun, W.K. Chen, S.H. Liu, M.J. Cao, C.H. Lu, Y. Xu, Chin. J. Inorg. Chem. 22 (2006) 1215.